UBC13-mediated template switching promotes replication stress resistance in FBH1-deficient cells

Alexandra L. Hawks[1#], Amy Bergmann[1#], Tyler J. McCraw[1], and Jennifer M. Mason[1*]

[1]Department of Genetics and Biochemistry, Clemson University, Clemson University

# Equal contribution

Keywords: FBH1, replication stress, template switching, UBC13, RAD51

*To whom correspondence should be addressed:

Jennifer M. Mason, Ph.D.
Department of Genetics and Biochemistry
Clemson University
130 McGinty Court
154 Poole
Clemson, SC 29634
Email address: jmason4@clemson.edu

ABSTRACT

The proper resolution of DNA damage during replication is essential for genome stability. FBH1, a UvrD, helicase plays crucial roles in the DNA damage response. FBH1 promotes double strand break formation and signaling in response to prolonged replication stress to initiate apoptosis. Human FBH1 regulates RAD51 to inhibit homologous recombination. A previous study suggested that mis-regulation of RAD51 may contribute to replication stress resistance in FBH1-deficient cells, but the underlying mechanism remains unknown. Here, we provide direct evidence that RAD51 promotes replication stress resistance in FBH1-deficient cells. We demonstrate inhibition of RAD51 using the small molecule, B02, partially rescues double strand break signaling in FBH1-deficient cells. We show that inhibition of only the strand exchange activity of RAD51 rescues double strand break signaling in FBH1 knockout cells. Finally, we show that depletion of UBC13, a E2 protein that promotes RAD51-dependent template switching, rescues double strand break formation and signaling sensitizing FBH1-deficient cells to replication stress. Our results suggest FBH1 regulates template switching to promote replication stress sensitivity.

INTRODUCTION

DNA must be accurately replicated each cell cycle to maintain the integrity of the genome. Replication stress caused by depletion of nucleotide pools, collision between replication and transcription machinery, or DNA damage slows and/or stalls replication forks threatening genome stability[1]. In response to replication stress, cells activate the DNA damage response that includes cell cycle checkpoints and DNA repair pathways. Defects in the replication stress response increase genome instability and contribute to human disease such as cancer[2,3].

Upon replication fork stalling, fork regression occurs by re-annealing nascent DNA strands to convert a replication fork from a 3-way junction to a 4-way junction[4]. There are multiple proteins that mediate fork regression in cells and function in at least two independent pathways. HLTF, SMARCAL1, and ZRANB3 function in one pathway, and FBH1 functions in the second pathway[5–11]. RAD51 is required for fork regression in both the HLTF- and FBH1-dependent pathways[12,13]. RAD51 is stabilized on the regressed arm to protect the newly synthesized DNA from degradation by nucleases including MRE11[14,15]. Therefore, fork regression is proposed to maintain genome integrity by preventing nucleolytic degradation of replication forks.

Other DNA damage tolerance pathways including translesion synthesis (TLS), PRIMPOL-mediated repriming, and template switching function in the response to replication stress. Emerging evidence indicates fork regression also limits replication progression in response to stresses by inhibiting TLS and PRIMPOL-mediated repriming. TLS polymerases such as Polη and Polκ are recruited to stalled replication forks after proliferating cell nuclear antigen (PCNA) mono-ubiquitination at lysine-164 by RAD18[16]. TLS polymerases can bypass lesions allowing replication to continue even in the presence of damage. PRIMPOL uses primase

activity to reprime downstream of the replication fork and performs DNA synthesis for a few nucleotides[17]. PRIMPOL is then dissociated from the DNA to allow the replicative polymerases to continue DNA synthesis. PRIMPOL can be used to bypass UV lesions and bulky lesions to complete DNA replication[17,18]. Fork regression mediated by HLTF, RAD51, and SMARCAL1 prevents PRIMPOL-mediated repriming at stalled replication forks[10,19–21]. Increased PRIMPOL activity contributes to cisplatin resistance in BRCA1-deficient cells[19]. In addition to TLS and PRIMPOL-mediated repriming, template switching functions at replication forks. RAD51-dependent template switching uses the complementary sister chromatid to extend the nascent ssDNA resulting in lesion bypass[22]. PCNA polyubiquitination at lysine-164 by UBC13, MMS2 and HLTF/SHPRH promotes template switching[23–26]. The ssDNA gaps left by PRIMPOL are repaired by post-replication repair pathways including TLS during S and G2 phase or template switching during S phase[21].

These studies demonstrate that fork reversal plays an important role in regulating TLS and PRIMPOL-mediated repriming, but we do not fully understand how template switching is regulated at stalled replication forks in human cells. In *S. cerevisiae*, SUMOylation of PCNA inhibits homologous recombination (HR) in S phase by recruiting the anti-recombinase Srs2 resulting in disassembly of Rad51 presynaptic filaments[27–30]. In *S. pombe,* Srs2 and Fbh1 suppress Rad51-mediated homologous recombination at stalled replication forks inhibiting template switching-dependent replication restart[31–33]. However, human FBH1 inhibition of template switching at stalled replication forks has not been thoroughly addressed.

FBH1 is a UvrD helicase with 3'-5' activity that functions in response to replication stress[34,35]. FBH1 promotes MUS81-dependent cleavage of stalled replication forks in response to prolonged treatment with hydroxyurea (HU) and ultra-violet (UV) radiation[36,37]. Hemizygous or

homozygous loss of FBH1 was found in up to 63% of cell lines derived from metastatic melanoma[38]. Furthermore, FBH1 protects melanocytes from UV-mediated malignant transformation suggesting FBH1 plays an important role in preventing tumorigenesis. However, how FBH1 promotes MUS81-dependent cleavage of stalled replication forks is not clear.

To date, there have been two proposed mechanisms for how FBH1 promotes double strand break (DSB) formation and cell death in response to prolonged replication stress. First, FBH1 mediates fork regression in response to HU[8]. In this instance, the absence of fork regression can lead to increased PRIMPOL-mediated repriming or TLS as seen in HLTF-deficient cells[10]. Second, FBH1 is unique among the fork remodeling enzymes because FBH1 inhibits HR by disassembling RAD51 presynaptic filaments from ssDNA[39–42]. FBH1 contains an FBOX that interacts with SKP1 to form a SKP1-CUL1-FBOX (SCF) protein complex that functions as an E3 ubiquitin ligase[34,35]. After FBH1 removes RAD51 from ssDNA, the SCF^{FBH1} ubiquitinates RAD51 to prevent reassociation of RAD51 with DNA[34,35,40]. Expression of a ubiquitination-resistant mutant of RAD51, RAD51 K58/64R, results in reduced DSB formation and increased survival in response to HU, suggesting that the ability of FBH1 to regulate RAD51 may be important for promoting sensitivity to replication stress[42]. Whether RAD51 is contributing to resistance in FBH1-deficient cells has not been directly tested.

In this study, we aimed to elucidate whether RAD51 plays a role in promoting resistance to replication stress in FBH1-deficient cells. We demonstrated inhibition of RAD51 restores DSB signaling in FBH1-deficient cells after prolonged exposure to HU. Specifically, inhibition of the strand exchange of RAD51 (i.e., HR) rescued DSB signaling in FBH1-deficient cells, Finally, we determined that knockdown of UBC13, a protein that promotes template switching, rescued DSB signaling and sensitized FBH1-deficient cells to replication stress. Together, our

data suggests that FBH1 regulates template switching to promote replication stress sensitivity and that inhibition of template switching may be a potential strategy for targeting FBH1-deficient tumors.

MATERIAL AND METHODS

Cell lines.

U2OS cell lines were cultured in Dulbecco's Modified Eagle's Medium (DMEM) supplemented with 10% FBS. RPE-1 cells were cultured in DMEM/F-12 media supplemented with 10% FBS. All cells were cultured at 37ºC with 5% CO_2. The U2OS FBH1-KO cell line was generated using CRISPR-Cas9 technology.

RNA Interference

Cells ($1.0\text{-}1.5 \times 10^5$) were plated in 6-well plates. After 24 hours, cells were transfected with siRNAs using Lipofectamine RNAiMax (Invitrogen) following the manufacturer's instructions. The siFBH1 final concentration was 75 nM[13]. The siUBC13 siRNA final concentration was 50 nM[21]. The All-Star negative control siRNA (Qiagen) was used as a control. Cells were replated for assays 24 hours after the transfection.

Drug Treatments

B02 was and RI(dl)2 were resuspended in DMSO and stored at -20ºC. Hydroxyurea was resuspended in UltraPure dH_2O and used immediately. Cells were treated either 24 hours following plating or 48 hours following siRNA transfection. DMSO or indicated concentrations of B02 and RI(dl)2 was added to the cells 30 minutes prior to the addition of hydroxyurea. Cells

were treated with 2 mM hydroxyurea for 24 hours with or without DMSO or indicated concentrations of B02 and RI(dl)2.

Generation of FBH1 polyclonal antibodies

The N-terminal 250 amino acids of human FBH1 were cloned in to a pGEX6p-1 expression vector using Gibson assembly. Primers used to amplify the FBH1 fragment were FBH1_pGEX6_F (5' TTCTGTTCCAGGGGCCCCTGGGATCCagctacgaggtgacttcag) and FBH1_N250_pGEX__R (5' GTCGACCCGGGAATTCCGGGGATCCtcaaagcccatagtatgagtcag). GST-FBH1[1-250] in the pGEX6P-1 vector (Amersham/GE Healthcare/Cytiva) was introduced into BL21:DE3 Rosetta cells (Novagen). The cells were grown at 37 °C to an OD_{600} of 0.8 and induced with 0.4 mM IPTG for 16 h at 16 °C. All the steps of the purification were performed at 4 °C. A 10 g pellet of cells was suspended in 50 mL of cell breakage buffer (50 mM Tris-HCl, pH 7.5, 10% sucrose, 2 mM EDTA, 250 mM KCl, 0.01% IgePal, 1 mM DTT, 1 mM Phenylmethulsulfonyl fluoride, 0.5 mM benzamidine and 5 μg/mL each of aprotinin, chymostatin, leupeptin, and pepstatin). The cells were sonicated and the crude lysate was centrifuged at 100,000 x g for 90 min. The clarified lysate was incubated with 1 mL of glutathione Sepharose (Cytiva) with constant agitation. The matrix was poured into a 1 cm column and washed with 10 mLs Buffer A (50 mM Tris-HCl, pH8.0, 10% glycerol, 1 mM EDTA, 1 mM DTT, and 0.01% IgePal) containing 1 M KCl and then 5 mL of Buffer A containing 300 mM KCl. The bound GST-FBH1[1-250] was eluted with 6 mL of 10 mM glutathione in Buffer A containing 300 mM KCl. The fractions containing GST-FBH1[1-250] were pooled and concentrated in an Amicon Ultra microconcentrator to 500 μL and subjected to size exclusion chromatography on a 40 mL Sephacryl S200 column in Buffer A containing 300

mM KCl. The fractions containing GST-FBH1[1-250] were pooled and concentrated as before to 8 mg/mL, and stored in small aliquots at -80 °C. ~1 mg of GST-FBH1[1-250] was used to generate antibodies from Pacific Immunology. Purified GST-FBH1[1-250] was coupled to CNBr activated Sepharose per the manufacturer's instructions. Serum was applied to a 1 mL of the matrix in a 1 cm column. The matrix was washed with 10 mL PBS (10 mM Na_2HPO_4, pH 7.4, 2.7 mM KCl, 137 mM NaCl, 0.05 % TWEEN) followed by elution with 166 mM MES pH 6.0 containing 100 mM diethylamine. The fractions that contained the antibodies were pooled and dialyzed against PBS. The dialyzed antibodies were concentrated in a Amicon Ultra microconcentrator, supplemented with 0.01% sodium azide and stored in small aliquots at 4 °C.

Immunoblotting

Cells were lysed by resuspending pellets in 100 µL 1:1 2xSDS:1xPBS per $1x10^6$ cells and boiled for 5 minutes. Denatured proteins were run on an SDS-PAGE gel and transferred to PVDF membrane. Membranes were probed with primary antibodies (diluted in 5% milk in 1xTBST) for 1 hour at room temperature to overnight at 4ºC. The membrane washed three times with 1xTBST and probed with HRP-conjugated secondary antibodies (WesternSure, Licor) for one hour at room temperature. Membrane was washed three times with 1xTBST, incubated with 1:1 ECL reagents for 5 minutes at room temperature, and imaged using a Licor C-Digit scanner. The primary antibodies used were FBH1 (1:500), Alpha-tubulin (Novus Biologicals, NB100-690,1:1000), UBC13 (Santa Cruz, Sc376470, 1:1000), and Vinculin (Cell Signaling Technologies,13901S 1:1000).

Immunofluorescence

Cells ($5.0x10^4$) plated on glass coverslips in 12-well plates one day prior to drug treatment. Following the drug treatment, cells were washed with PBS and incubated in HEPES/TritonX-100 Buffer (20 mM HEPES, ph7.4, 0.5% Triton-X 100, 50mM NaCl, 3 mM MgCl2, 300 mM sucrose in water) for 10 minutes at room temperature. Cells were fixed with 3% paraformaldehyde, 3.4% sucrose in 1xPBS for 10 minutes at room temperature. Cells were washed twice with 1xPBS. For PCNA staining, cells were treated with ice cold 100% Methanol for 10 minutes followed by two additional PBS washes. Cells were incubated with 1% BSA in 1xPBS for 20 minutes at room temperature. Cells were incubated with the primary antibodies (diluted in 1% BSA) for 1 hour at room temperature or overnight at 4°C and were washed three times with 1xPBS. Coverslips were incubated with the secondary antibodies (diluted in 1% BSA) for 1 hour at room temperature away from light and were washed 3 times with 1xPBS. Once dry, coverslips were mounted with Vectashield + DAPI and sealed with nail polish. Images acquired on Zeiss Axio M2 upright fluorescence microscope and data quantified using ImageJ software. The primary antibodies used were Mouse anti-RPA32/RPA2 [9H8] (Abcam Ab2175, 1:1000), Rabbit phospho-RPA32 (Ser33) polyclonal (Bethyl Laboratories, A300-246A-T,1:1000), Rabbit phospho-RPA32 (Ser4, Ser8) polyclonal (Bethyl Laboratories, A300-245A-M, 1:1000), Rabbit anti-PCNA (Abcam, Ab18197, 1:1000), and Mouse anti-gamma H2AX (phospho S139) [9F3] (Abcam, Ab26350, 1:1000).

TUNEL Assay

TUNEL assay performed using Click-IT Plus TUNEL assay kit (Invitrogen) following manufacturer's protocol. All incubations longer than 5 minutes were performed in a humidity

chamber. Cells were lysed and fixed as described above. Coverslips were incubated with TdT Reaction Buffer for 10 minutes at 37ºC. Excess buffer was removed, and the TdT reaction mixture (TdT Reaction Buffer, EdUTP, and TdT Enzyme) was added to each coverslip. Coverslips were incubated for 60 minutes at 37ºC. Coverslips were rinsed once with dH_2O, followed by a 5-minute wash with 3% BSA, 0.1% Triton X-100 in 1xPBS for 5 minutes at room temperature. Coverslips are rinsed with 1xPBS and incubated with Click-iT PLUS TUNEL Reaction cocktail (Click-iT supermix, 10x Click-iT Additive) for 30 minutes at 37ºC. Coverslips washed with 3% BSA in 1xPBS for 5 minutes, followed by a rinse with 1xPBS. Slides were next stained for PCNA as the cell cycle indicator using protocol described previously.

Survival Assay

Cells were plated in 96-well black, clear bottom plates (Corning) 24 hours post-transfection. 100-500 cells plated per well in triplicate. 48 hours post-transfection cells were treated with 0-4 mM HU for 24 hours. Following treatment, cells were washed twice with 1xPBS and allowed to recover in fresh media for 4-5 days. 20 µL of CellTiter-Blue reagent was added to each well containing cells plus 3 no-cell control wells and incubated at 37ºC for 2 hours. The reaction was stopped by adding 50 µL of 3% SDS to each well. On a Synergy H1 plate reader, plates were shaken for 10 seconds, and endpoint fluorescence read at 570/600. Fluorescence data used to quantify survival of each sample.

Quantification and Statistical Analysis

All microscopy images were scored using ImageJ software. Statistical analysis was performed using Prism software, and the tests performed are indicated in figure legends. All experiments consist of three independent experiments.

RESULTS

Inhibition of RAD51 partially restored double strand break signaling in FBH1-deficient cells.

Expression of RAD51-K58/64R, a mutant that is resistant to ubiquitylation by FBH1, results in increased HR activity, reduced DSB formation, and increased survival following replication stress suggesting that mis-regulation of RAD51 is contributing to replication stress resistance in FBH1-defcient cells[42]. We aimed to determine how RAD51 is contributing to replication stress resistance in FBH1-deficient cells by testing the impact of RAD51 inhibition on the cellular response to HU in FBH1-deficient cells. To do this, we knocked out FBH1 in U2OS cells (hereafter FBH1 KO) and verified loss of FBH1 by western blotting (**Supplemental Figure 1A**).

First, we treated U2OS and FBH1 KO cells with 2 mM HU for 24 hours with or without the RAD51 inhibitor, B02, which inhibits the DNA binding activity of RAD51 and examined induction of the replication stress response[43]. When replication forks stall, RPA bound to ssDNA at stalled forks is phosphorylated at serine-33 (pRPA S33) by the ATR kinase[44]. We quantified pRPA S33 in RPA positive cells following treatment with HU and B02 in U2OS cells. We found no significant difference in the percentage of pRPA S33 positive cells between U2OS and FBH1 KO cells (**Figure 1A**). The addition of B02 caused no significant change in the percentage of pRPA S33 positive cells in U2OS or FBH1 KO cells. This result indicates

treatment with B02 does not significantly alter the replication stress response in U2OS and FBH1 KO cells.

Next, we determined if inhibition of RAD51 with B02 restored double strand break signaling in FBH1-deficient cells after HU treatment. Prolonged replication stress after HU treatment results in excessive ssDNA accumulation, ultimately exhausting the cellular pool of RPA[45]. The exposed ssDNA is susceptible to cleavage by nucleases including MUS81[46]. After end resection, RPA binds to the ssDNA overhangs and is phosphorylated at serines 4 and 8 (pRPA S4/8) by DNAPkcs and can be quantified using fluorescence microscopy[47]. After HU treatment, 63% of RPA positive U2OS cells were pRPA S4/8 positive and B02 treatment results in a small, but significant increase in pRPA S4/8 positive cells (**Figure 1B**). As reported previously, FBH1-deficient cells exhibited a 2.4-fold reduction in pRPA S4/8 positive cells compared to U2OS cells consistent with a defect in DSB signaling after HU treatment[36,37]. Treatment of FBH1 KO cells with 10 and 25 μM B02 significantly increased pRPA S4/8 positive cells to 46% and 48%, respectively compared to FBH1 KO cells (**Figure 1B)**. This result suggests inhibition of RAD51 partially restored DSB signaling in FBH1-deficient cells.

In response to DNA damage, the histone variant, H2AX, is phosphorylated at serine-139[48]. Intensive, uniform γ-H2AX staining (i.e., pan-nuclear γ-H2AX) has been associated with replication catastrophe[45]. Previous studies have shown FBH1-deficient cells exhibit a significant reduction in pan-nuclear γ-H2AX following prolonged replication stress[36,37]. We determined if B02 treatment restored induction of pan-nuclear γ-H2AX after treatment with 2 mM HU. Cells were co-stained with PCNA to identify cells in S phase at the time of HU treatment. In U2OS cells, 32% of PCNA positive U2OS cells were positive for pan-nuclear γ-H2AX staining and B02 treatment did not significantly change the percentage of cells containing pan-nuclear γ-

H2AX. As expected, FBH1 KO cells had a 5-fold reduction in the percentage of cells with pan-nuclear γ-H2AX staining compared to U2OS cells (7% compared to 32%) (**Figure 1C**). FBH1 KO cells treated with 10 and 25 μM B02 and 2 mM HU had 19% and 31% pan-nuclear γ-H2AX positive cells, respectively. These data suggest that inhibition of RAD51 partially restores DNA damage signaling in FBH1-deficient cells after HU treatment.

Inhibition of the strand exchange activity of RAD51 rescues DSB signaling in FBH1 KO cells.

We reasoned there are at least two potential mechanisms by which RAD51 inhibition could restore DSB signaling in FBH1-deficient cells. First, RAD51 nucleoprotein filaments can inhibit MUS81 cleavage[49,50]. FBH1 may be removing RAD51 from DNA to allow MUS81 to access stalled forks. We hypothesized if RAD51 bound to DNA was preventing MUS81 cleavage, inhibition of RAD51 strand exchange (e.g. HR) would not restore DSB signaling in FBH1-deficient cells. Second, similar to yeast Fbh1, human FBH1 may be inhibiting HR at stalled replication forks[27–30] and would require the strand exchange of RAD51. To distinguish between these two mechanisms, we treated cells with the inhibitor, RI(dl)2, that inhibits the strand exchange activity of RAD51. During HR, RAD51 forms a nucleoprotein filament on ssDNA using site I and performs homology search and strand exchange using site II binding site. In yeast and humans, mutations in site II result in a RAD51 mutant capable of forming presynaptic filaments, but deficient in carrying out recombination[13,51]. The small molecule, RI(dl)2, mimics a site II mutant by inhibiting the strand exchange of RAD51 without disrupting RAD51 nucleoprotein filament formation[52].

To determine if inhibition of HR restored DSB signaling in FBH1 KO cells, we treated cells with 2 mM HU for 24 hours with or without the inhibitor, RI(dl)2, and examined induction of pRPA S33. We observed no significant change in pRPA S33 staining in U2OS or FBH1 KO cells with either 25 or 50 μM RI(dl)2 (**Figure 2A**). This suggests that the inhibition of the strand exchange activity of RAD51 does not have a significant impact on induction of the replication stress response in U2OS and FBH1 KO cells.

Next, we determined whether inhibition of the strand exchange activity of RAD51 had any impact on DSB signaling in FBH1-deficient cells. U2OS and FBH1 KO cells were treated with 2 mM HU with or without RI(dl)2 for 24 hours. In U2OS cells, 66% of RPA positive cells were positive for pRPA S4/8 (**Figure 2B).** Treating U2OS cells with RI(dl)2 did not significantly change the percent of RPA positive cells with pRPA 4/8 signaling, indicating RI(dl)2 treatment alone is not impacting induction of DSB signaling. FBH1 KO cells had a 2-fold decrease in pRPA S4/8 positive cells compared to U2OS. Treating FBH1 KO cells with 25 μM RI(dl)2 significantly increased pRPA S4/8 positive cells to 61% compared to the FBH1 KO. When treated with 50μM RI(dl)2, FBH1 KO cells exhibited induction of pRPA S4/8 similar to U2OS cells with 72% of RPA positive cells containing pRPA S4/8. This result suggests that inhibition of strand exchange activity of RAD51 restores DSB signaling in FBH1-deficient cells after HU treatment.

UBC13 knockdown restores DSB signaling in FBH1-deficient cells.

As inhibition of the strand exchange activity of RAD51 restored DSB signaling, we next asked if inhibition of template switching, a DDT pathway that requires the strand exchange activity of RAD51 at stalled replication forks, restored DSB signaling in FBH1-deficient cells[53].

The E2 protein, UBC13, works with SHRPH to contribute to polyubiquitination of PCNA at lysine 164 to promote RAD51-dependent template switching[23,54]. We depleted UBC13 from U2OS and FBH1 KO cells using siRNAs (**Supplemental Figure 1B**). Cells were then treated for 24 hours with 2 mM HU and stained for the DSB marker pRPA S4/8. U2OS cells had approximately 70% of RPA positive cells that were also positive for pRPA S4/8 and knockdown of UBC13 did not result in a significant difference in the percentage of pRPA S4/8 cells (**Figure 3A**). In FBH1 KO cells, we observed a 2-fold decrease in pRPA S4/8 positive cells compared to the non-silencing control in U2OS (siNS). When UBC13 was knocked down in FBH1 KO cells, we observed a significant increase in the percentage of pRPA S4/8 cells from 37% to 69%. We observed a similar result when we examined pan-nuclear γ–H2AX in U2OS and FBH1 KO upon UBC13 knockdown (**Figure 3B**). Compared to U2OS, FBH1 KO cells exhibited a 4-fold decrease in pan-nuclear γ–H2AX positive cells. When UBC13 was depleted in FBH1 KO cells, the percentage of pan-nuclear γ–H2AX positive cells increased from 9% to 28% indicating depletion of UBC13 rescues DSB signaling defect in FBH1-deficient cells.

Next, we determined if depletion of UBC13 would rescue DSB signaling in siFBH1 transfected RPE-1 cells. RPE-1 cells transfected with the non-silencing control (siNS) contained 66% RPA positive cells that were also pRPA S4/8 positive and knockdown of UBC13 alone (siUBC13) did not significantly change the percentage of pRPA S4/8 cells (**Supplemental Figure 2A**). Like U2OS cells, FBH1-depleted cells (siFBH1) exhibited a significant reduction in pRPA S4/8 positive cells (24%) and knocking down UBC13 increased pRPA positive cells to 53%. We observed a similar result when we examined pan-nuclear γ–H2AX in RPE-1 cells (**Supplemental Figure 2B**). Cells transfected with siNS exhibited 34% of γ–H2AX positive cells and UBC13 knockdown did not significantly change the percentage of cells containing pan-

nuclear γ–H2AX. Knockdown of FBH1 reduced the percentage of cells with pan-nuclear γ–H2AX to 6% and knockdown of UBC13 rescued induction of pan-nuclear γ–H2AX (34%). Together, these results indicated depletion of UBC13 rescues DSB signaling in FBH1-deficient cells.

UBC13 knockdown rescues DSB formation in FBH1-deficient cells.

FBH1 works with MUS81 to promote DSB formation in response to prolonged replication stress[36]. FBH1-deficient cells exhibit a significant reduction in DSBs after prolonged HU treatment. To determine if depletion of UBC13 rescues DSB formation in FBH1-deficient cells, U2OS and FBH1 KO cells were treated for 24 hours with 2 mM HU and DSBs were detected using the TUNEL assay that has been previously shown to detect excessive breakage due to replication catastrophe[45]. After HU treatment, depletion of UBC13 in U2OS cells resulted in a slight decrease in TUNEL positive cells from 32% to 27% (**Figure 4A**). In FBH1 KO cells, we observed a significant decrease in TUNEL positive cells (1%) compared to U2OS cells. When we depleted UBC13 in FBH1 KO cells, the TUNEL positive cells increased to 25%. A similar result was observed in RPE-1 cells depleted of UBC13 and FBH1 (**Figure 4B**). Compared to siNS-transfected cells, FBH1-depleted cells exhibited a 17-fold reduction in TUNEL positive cells. Depletion of UBC13 in siFBH1-transfected cells increased the percentage of TUNEL positive cells from 2% to 26%. Taken together, these results indicate that inhibition of UBC13 restores DSB formation and signaling in FBH1-deficient cells treated with HU.

UBC13 sensitizes FBH1-deficient cells to HU.

In FBH1-deficient cells, reduced DSB break formation results in increased resistance to HU[36,37]. Given UBC13 depletion restored DSB formation and signaling in FBH1-deficient cells, we next determined if UBC13 depletion restored sensitivity of FBH1-deficient cells to HU. We treated cells with increasing amounts of HU and measured cell survival. As expected, FBH1 KO cells had increased survival compared to U2OS consistent with FBH1 KO cells being resistant to replication stress (**Figure 5**). Depletion of UBC13 in U2OS cells had no significant impact on cell survival in response to HU. Importantly, when UBC13 was knocked down in FBH1 KO cells, there was a significant decrease in survival compared to the FBH1 KO cells. Together, these data suggest that inhibition of UBC13 sensitizes FBH1-deficient cells to replication stress by restoring DSB formation.

DISCUSSION

FBH1 is an anti-recombinase that inhibits HR by removing RAD51 from ssDNA at stalled replication forks[39–41]. As part of the SCF^{FBH1} complex, FBH1 mediates the ubiquitination of RAD51 to prevent reassociation with DNA[34,35,40]. Over-expression of a ubiquitination resistant RAD51 mutant resulted in decreased DSB formation and increased resistance to HU suggesting regulation of RAD51 by FBH1 is important to promote sensitivity to replication stress[41]. However, it is not known if K58/K64R disrupted functions of RAD51 as the biochemical activities of RAD51 K58/K64R were not tested. Here, we provide direct evidence that inhibition of RAD51 filament assembly or strand exchange restores DSB signaling in FBH1-deficient cells after HU treatment. In addition, we demonstrate depletion of UBC13 restores DSB signaling and sensitizes FBH1-deficient cells to replication stress. Together, these results indicate loss of template switching restores replication stress sensitivity in FBH1-deficient cells.

RAD51 nucleoprotein filaments bound to stalled replication forks can inhibit MUS81 access to DNA preventing DSB formation[49,50]. The anti-recombinases yeast Srs2 and human RECQ5 have been shown to remove RAD51 from DNA to promote MUS81 cleavage. Thus, one possibility is that FBH1 removes RAD51 from stalled replication forks to promote MUS81-dependent DSB formation. Consistent with this model, inhibition of RAD51 filament assembly resulted in partial rescue of DSB signaling after prolonged HU treatment in FBH1 KO cells. We predicted that if this was the primary mechanism of replication stress resistance in FBH1-deficient cells, inhibition of strand exchange activity of RAD51 without disruption of RAD51 nucleofilament assembly would not restore DSB signaling. However, our data suggest that inhibiting the strand exchange activity of RAD51 or depleting UBC13 restores levels of DSBs signaling and sensitivity in FBH1-deficient cells to levels observed in U2OS cells indicating the primary mechanism underlying replication stress resistance in FBH1-deficient cells involves HR.

UBC13 is an ubiquitin E2 conjugating enzyme that forms polyubiquitin chains with different E3 enzymes in multiple cellular pathways including TRAF-mediated inflammatory response, DSB repair and template switching[55–58]. UBC13 polyubiquitinates PCNA to promote RAD51-dependent template switching[55]. Our results indicate that depletion of UBC13 sensitizes FBH1 KO cells to HU. Given inhibition of the strand exchange of RAD51 also restores DSB signaling in FBH1-deficient cells, we propose inhibition of template switching is sensitizing FBH1-deficient cells to HU. Template switching restarts stalled replication forks, bypasses DNA lesions and fills ssDNA gaps during S phase[21,32,59]. One possibility is that the anti-recombinase activity of FBH1 disassembles RAD51 presynaptic filaments to inhibit template switching. In *S. pombe*, Fbh1 plays a similar role inhibiting HR at stalled replication forks[30,31,60,61]. Indeed, upregulation of RAD51 and template switching can lead to resistance to chemotherapeutics[62–65].

Alternatively, FBH1-deficient cells may depend on UBC13-mediated template switching in response to replication stress. Previous studies have shown that PRIMPOL-mediated DNA synthesis is upregulated in cells lacking fork regression mediated by HLTF, RAD51 and SMARCAL1[19–21]. Excessive PRIMPOL activity promotes resistance to replication stress in a BRCA1-deficient background[66]. The resulting ssDNA gaps left by PRIMPOL can be filled by template switching during S phase[21]. FBH1 promotes fork regression in an HLTF-independent pathway[8,12]. Therefore, it is possible FBH1 KO cells are reliant on template switching to fill ssDNA gaps that arise due to PRIMPOL-dependent synthesis due to the defect in fork regression. Future work is warranted to distinguish between these models.

Hemizygous and homozygous loss of FBH1 was found in up to 63% of cell lines derived from melanoma. FBH1 protects melanocytes from UV-mediated transformation and FBH1-deficient melanoma cell lines are resistant to replication stress induced by HU[38]. Our results here suggest UBC13-dependent template switching may be a potential target to sensitize FBH1-deficient tumors to replication stress. Future studies will determine if template switching is driving UV resistance and malignant transformation of melanocytes.

Limitations of Study

Finally, there are limitations to the current study. First, we were unable to directly test the role of the anti-recombinase activity of FBH1 in promoting resistance to HU. Mutations in FBH1 that disrupt the anti-recombinase activity of FBH1 disrupt other functions. The helicase activity of FBH1 is required for both the anti-recombinase activity of FBH1 and to promote fork regression[8,39,41]. Ubiquitination of RAD51 to prevent re-associated of DNA after removal by FBH1 requires the FBOX; however, FBH1 is also ubiquitinated to negatively regulate anti-

recombinase activity[40,42]. Second, inhibition of RAD51 and UBC13 is inhibiting other pathways besides template switching. These limitations highlight the need for generation of a separation-of-function mutant that disrupts only the anti-recombinase activity of FBH1.

AUTHOR CONTRIBUTIONS

ALH, AB, and JMM designed the project. ALH, AB, and TJM conducted the experiments and analyzed data. JMM supervised the project. The manuscript was written by ALH, AB, and JMM.

DATA AVAILABILITY

Further information and requests for resources and reagents should be directed to and will be fulfilled by the lead contact, Jennifer Mason, PhD (jmason4@clemson.edu). All data will be available upon request.

FUNDING

This work is funded in part by the American Cancer Society Research Scholar Grant RSG-21-175-01-DMC (https://doi.org/10.53354/pc.gr.152677) to J.M.M and NIGMS (R35 GM142512-01) to J.M.M.

ACKNOWLEDGEMENTS

We would like to thank Garrett Buzzard and Michael Sehorn for purification of GST-tagged FBH1-N250 and FBH1 polyclonal antibodies. We thank Michael Sehorn for feedback on a draft of the manuscript.

REFERENCES

1. Zeman, M.K., and Cimprich, K.A. (2014). Causes and consequences of replication stress. Nat Cell Biol *16*, 2–9. 10.1038/ncb2897.

2. Muñoz, S., and Méndez, J. (2017). DNA replication stress: from molecular mechanisms to human disease. Chromosoma *126*, 1–15. 10.1007/s00412-016-0573-x.

3. Fitzgerald, D.M., Hastings, P.J., and Rosenberg, S.M. (2017). Stress-Induced Mutagenesis: Implications in Cancer and Drug Resistance. Annu. Rev. Cancer Biol. *1*, 119–140. 10.1146/annurev-cancerbio-050216-121919.

4. Fujiwara, Y., and Tatsumi, M. (1976). Replicative bypass repair of ultraviolet damage to DNA of mammalian cells: Caffeine sensitive and caffeine resistant mechanisms. Mutation Research/Fundamental and Molecular Mechanisms of Mutagenesis *37*, 91–109. 10.1016/0027-5107(76)90058-0.

5. Zellweger, R., Dalcher, D., Mutreja, K., Berti, M., Schmid, J.A., Herrador, R., Vindigni, A., and Lopes, M. (2015). Rad51-mediated replication fork reversal is a global response to genotoxic treatments in human cells. Journal of Cell Biology *208*, 563–579. 10.1083/jcb.201406099.

6. Weston, R., Peeters, H., and Ahel, D. (2012). ZRANB3 is a structure-specific ATP-dependent endonuclease involved in replication stress response. Genes Dev. *26*, 1558–1572. 10.1101/gad.193516.112.

7. Kile, A.C., Chavez, D.A., Bacal, J., Eldirany, S., Korzhnev, D.M., Bezsonova, I., Eichman, B.F., and Cimprich, K.A. (2015). HLTF's Ancient HIRAN Domain Binds 3′ DNA Ends to Drive Replication Fork Reversal. Molecular Cell *58*, 1090–1100. 10.1016/j.molcel.2015.05.013.

8. Fugger, K., Mistrik, M., Neelsen, K.J., Yao, Q., Zellweger, R., Kousholt, A.N., Haahr, P., Chu, W.K., Bartek, J., Lopes, M., et al. (2015). FBH1 Catalyzes Regression of Stalled Replication Forks. Cell Reports *10*, 1749–1757. 10.1016/j.celrep.2015.02.028.

9. Vujanovic, M., Krietsch, J., Raso, M.C., Terraneo, N., Zellweger, R., Schmid, J.A., Taglialatela, A., Huang, J.-W., Holland, C.L., Zwicky, K., et al. (2017). Replication Fork Slowing and Reversal upon DNA Damage Require PCNA Polyubiquitination and ZRANB3 DNA Translocase Activity. Molecular Cell *67*, 882-890.e5. 10.1016/j.molcel.2017.08.010.

10. Bai, G., Kermi, C., Stoy, H., Schiltz, C.J., Bacal, J., Zaino, A.M., Hadden, M.K., Eichman, B.F., Lopes, M., and Cimprich, K.A. (2020). HLTF Promotes Fork Reversal, Limiting Replication Stress Resistance and Preventing Multiple Mechanisms of Unrestrained DNA Synthesis. Molecular Cell *78*, 1237-1251.e7. 10.1016/j.molcel.2020.04.031.

11. Kolinjivadi, A.M., Sannino, V., De Antoni, A., Zadorozhny, K., Kilkenny, M., Técher, H., Baldi, G., Shen, R., Ciccia, A., Pellegrini, L., et al. (2017). Smarcal1-Mediated Fork

Reversal Triggers Mre11-Dependent Degradation of Nascent DNA in the Absence of Brca2 and Stable Rad51 Nucleofilaments. Molecular Cell *67*, 867-881.e7. 10.1016/j.molcel.2017.07.001.

12. Liu, W., Krishnamoorthy, A., Zhao, R., and Cortez, D. (2020). Two replication fork remodeling pathways generate nuclease substrates for distinct fork protection factors. Sci. Adv. *6*, eabc3598. 10.1126/sciadv.abc3598.

13. Mason, J.M., Chan, Y.-L., Weichselbaum, R.W., and Bishop, D.K. (2019). Non-enzymatic roles of human RAD51 at stalled replication forks. Nat Commun *10*, 4410. 10.1038/s41467-019-12297-0.

14. Hashimoto, Y., Ray Chaudhuri, A., Lopes, M., and Costanzo, V. (2010). Rad51 protects nascent DNA from Mre11-dependent degradation and promotes continuous DNA synthesis. Nat Struct Mol Biol *17*, 1305–1311. 10.1038/nsmb.1927.

15. Schlacher, K., Christ, N., Siaud, N., Egashira, A., Wu, H., and Jasin, M. (2011). Double-Strand Break Repair-Independent Role for BRCA2 in Blocking Stalled Replication Fork Degradation by MRE11. Cell *145*, 529–542. 10.1016/j.cell.2011.03.041.

16. Zhang, S., Zhou, T., Wang, Z., Yi, F., Li, C., Guo, W., Xu, H., Cui, H., Dong, X., Liu, J., et al. (2021). Post-Translational Modifications of PCNA in Control of DNA Synthesis and DNA Damage Tolerance-the Implications in Carcinogenesis. Int. J. Biol. Sci. *17*, 4047–4059. 10.7150/ijbs.64628.

17. Bianchi, J., Rudd, S.G., Jozwiakowski, S.K., Bailey, L.J., Soura, V., Taylor, E., Stevanovic, I., Green, A.J., Stracker, T.H., Lindsay, H.D., et al. (2013). PrimPol Bypasses UV Photoproducts during Eukaryotic Chromosomal DNA Replication. Molecular Cell *52*, 566–573. 10.1016/j.molcel.2013.10.035.

18. Piberger, A.L., Bowry, A., Kelly, R.D.W., Walker, A.K., González-Acosta, D., Bailey, L.J., Doherty, A.J., Méndez, J., Morris, J.R., Bryant, H.E., et al. (2020). PrimPol-dependent single-stranded gap formation mediates homologous recombination at bulky DNA adducts. Nat Commun *11*, 5863. 10.1038/s41467-020-19570-7.

19. Quinet, A., Tirman, S., Jackson, J., Šviković, S., Lemaçon, D., Carvajal-Maldonado, D., González-Acosta, D., Vessoni, A.T., Cybulla, E., Wood, M., et al. (2020). PRIMPOL-Mediated Adaptive Response Suppresses Replication Fork Reversal in BRCA-Deficient Cells. Molecular Cell *77*, 461-474.e9. 10.1016/j.molcel.2019.10.008.

20. Vallerga, M.B., Mansilla, S.F., Federico, M.B., Bertolin, A.P., and Gottifredi, V. (2015). Rad51 recombinase prevents Mre11 nuclease-dependent degradation and excessive PrimPol-mediated elongation of nascent DNA after UV irradiation. Proc. Natl. Acad. Sci. U.S.A. *112*. 10.1073/pnas.1508543112.

21. Tirman, S., Quinet, A., Wood, M., Meroni, A., Cybulla, E., Jackson, J., Pegoraro, S., Simoneau, A., Zou, L., and Vindigni, A. (2021). Temporally distinct post-replicative repair

mechanisms fill PRIMPOL-dependent ssDNA gaps in human cells. Molecular Cell *81*, 4026-4040.e8. 10.1016/j.molcel.2021.09.013.

22. Branzei, D., and Foiani, M. (2007). Template Switching: From Replication Fork Repair to Genome Rearrangements. Cell *131*, 1228–1230. 10.1016/j.cell.2007.12.007.

23. Motegi, A., Liaw, H.-J., Lee, K.-Y., Roest, H.P., Maas, A., Wu, X., Moinova, H., Markowitz, S.D., Ding, H., Hoeijmakers, J.H.J., et al. (2008). Polyubiquitination of proliferating cell nuclear antigen by HLTF and SHPRH prevents genomic instability from stalled replication forks. Proc. Natl. Acad. Sci. U.S.A. *105*, 12411–12416. 10.1073/pnas.0805685105.

24. Hofmann, R.M., and Pickart, C.M. (1999). Noncanonical MMS2-Encoded Ubiquitin-Conjugating Enzyme Functions in Assembly of Novel Polyubiquitin Chains for DNA Repair. Cell *96*, 645–653. 10.1016/S0092-8674(00)80575-9.

25. Ulrich, H.D. (2000). Two RING finger proteins mediate cooperation between ubiquitin-conjugating enzymes in DNA repair. The EMBO Journal *19*, 3388–3397. 10.1093/emboj/19.13.3388.

26. Broomfield, S., Chow, B.L., and Xiao, W. (1998). *MMS2* , encoding a ubiquitin-conjugating-enzyme-like protein, is a member of the yeast error-free postreplication repair pathway. Proc. Natl. Acad. Sci. U.S.A. *95*, 5678–5683. 10.1073/pnas.95.10.5678.

27. Papouli, E., Chen, S., Davies, A.A., Huttner, D., Krejci, L., Sung, P., and Ulrich, H.D. (2005). Crosstalk between SUMO and Ubiquitin on PCNA Is Mediated by Recruitment of the Helicase Srs2p. Molecular Cell *19*, 123–133. 10.1016/j.molcel.2005.06.001.

28. Krejci, L., Van Komen, S., Li, Y., Villemain, J., Reddy, M.S., Klein, H., Ellenberger, T., and Sung, P. (2003). DNA helicase Srs2 disrupts the Rad51 presynaptic filament. Nature *423*, 305–309. 10.1038/nature01577.

29. Pfander, B., Moldovan, G.-L., Sacher, M., Hoege, C., and Jentsch, S. (2005). SUMO-modified PCNA recruits Srs2 to prevent recombination during S phase. Nature *436*, 428–433. 10.1038/nature03665.

30. Veaute, X., Jeusset, J., Soustelle, C., Kowalczykowski, S.C., Le Cam, E., and Fabre, F. (2003). The Srs2 helicase prevents recombination by disrupting Rad51 nucleoprotein filaments. Nature *423*, 309–312. 10.1038/nature01585.

31. Lorenz, A., Osman, F., Folkyte, V., Sofueva, S., and Whitby, M.C. (2009). Fbh1 Limits Rad51-Dependent Recombination at Blocked Replication Forks. Mol Cell Biol *29*, 4742–4756. 10.1128/MCB.00471-09.

32. Jalan, M., Oehler, J., Morrow, C.A., Osman, F., and Whitby, M.C. (2019). Factors affecting template switch recombination associated with restarted DNA replication. eLife *8*, e41697. 10.7554/eLife.41697.

33. Tsutsui, Y., Kurokawa, Y., Ito, K., Siddique, Md.S.P., Kawano, Y., Yamao, F., and Iwasaki, H. (2014). Multiple Regulation of Rad51-Mediated Homologous Recombination by Fission Yeast Fbh1. PLoS Genet *10*, e1004542. 10.1371/journal.pgen.1004542.

34. Kim, J.-H. (2004). SCFhFBH1 can act as helicase and E3 ubiquitin ligase. Nucleic Acids Research *32*, 2287–2297. 10.1093/nar/gkh534.

35. Kim, J., Kim, J.-H., Lee, S.-H., Kim, D.-H., Kang, H.-Y., Bae, S.-H., Pan, Z.-Q., and Seo, Y.-S. (2002). The Novel Human DNA Helicase hFBH1 Is an F-box Protein. Journal of Biological Chemistry *277*, 24530–24537. 10.1074/jbc.M201612200.

36. Fugger, K., Kit Chu, W., Haahr, P., Nedergaard Kousholt, A., Beck, H., Payne, M.J., Hanada, K., Hickson, I.D., and Storgaard Sørensen, C. (2013). FBH1 co-operates with MUS81 in inducing DNA double-strand breaks and cell death following replication stress. Nat Commun *4*, 1423. 10.1038/ncomms2395.

37. Jeong, Y.-T., Rossi, M., Cermak, L., Saraf, A., Florens, L., Washburn, M.P., Sung, P., Schildkraut, C.L., and Pagano, M. (2013). FBH1 promotes DNA double-strand breakage and apoptosis in response to DNA replication stress. Journal of Cell Biology *200*, 141–149. 10.1083/jcb.201209002.

38. Jeong, Y.-T., Cermak, L., Guijarro, M., Hernando, E., and Pagano, M. (2013). FBH1 protects melanocytes from transformation and is deregulated in melanomas. Cell Cycle *12*, 1128–1132. 10.4161/cc.24165.

39. Simandlova, J., Zagelbaum, J., Payne, M.J., Chu, W.K., Shevelev, I., Hanada, K., Chatterjee, S., Reid, D.A., Liu, Y., Janscak, P., et al. (2013). FBH1 Helicase Disrupts RAD51 Filaments in Vitro and Modulates Homologous Recombination in Mammalian Cells. Journal of Biological Chemistry *288*, 34168–34180. 10.1074/jbc.M113.484493.

40. Masuda-Ozawa, T., Hoang, T., Seo, Y.-S., Chen, L.-F., and Spies, M. (2013). Single-molecule sorting reveals how ubiquitylation affects substrate recognition and activities of FBH1 helicase. Nucleic Acids Research *41*, 3576–3587. 10.1093/nar/gkt056.

41. Fugger, K., Mistrik, M., Danielsen, J.R., Dinant, C., Falck, J., Bartek, J., Lukas, J., and Mailand, N. (2009). Human Fbh1 helicase contributes to genome maintenance via pro- and anti-recombinase activities. Journal of Cell Biology *186*, 655–663. 10.1083/jcb.200812138.

42. Chu, W.K., Payne, M.J., Beli, P., Hanada, K., Choudhary, C., and Hickson, I.D. (2015). FBH1 influences DNA replication fork stability and homologous recombination through ubiquitylation of RAD51. Nat Commun *6*, 5931. 10.1038/ncomms6931.

43. Huang, F., Motlekar, N.A., Burgwin, C.M., Napper, A.D., Diamond, S.L., and Mazin, A.V. (2011). Identification of Specific Inhibitors of Human RAD51 Recombinase Using High-Throughput Screening. ACS Chem. Biol. *6*, 628–635. 10.1021/cb100428c.

44. Vassin, V.M., Anantha, R.W., Sokolova, E., Kanner, S., and Borowiec, J.A. (2009). Human RPA phosphorylation by ATR stimulates DNA synthesis and prevents ssDNA accumulation during DNA-replication stress. Journal of Cell Science *122*, 4070–4080. 10.1242/jcs.053702.

45. Toledo, L.I., Altmeyer, M., Rask, M.-B., Lukas, C., Larsen, D.H., Povlsen, L.K., Bekker-Jensen, S., Mailand, N., Bartek, J., and Lukas, J. (2013). ATR Prohibits Replication Catastrophe by Preventing Global Exhaustion of RPA. Cell *155*, 1088–1103. 10.1016/j.cell.2013.10.043.

46. Regairaz, M., Zhang, Y.-W., Fu, H., Agama, K.K., Tata, N., Agrawal, S., Aladjem, M.I., and Pommier, Y. (2011). Mus81-mediated DNA cleavage resolves replication forks stalled by topoisomerase I–DNA complexes. Journal of Cell Biology *195*, 739–749. 10.1083/jcb.201104003.

47. Ashley, A.K., Shrivastav, M., Nie, J., Amerin, C., Troksa, K., Glanzer, J.G., Liu, S., Opiyo, S.O., Dimitrova, D.D., Le, P., et al. (2014). DNA-PK phosphorylation of RPA32 Ser4/Ser8 regulates replication stress checkpoint activation, fork restart, homologous recombination and mitotic catastrophe. DNA Repair *21*, 131–139. 10.1016/j.dnarep.2014.04.008.

48. Rogakou, E.P., Pilch, D.R., Orr, A.H., Ivanova, V.S., and Bonner, W.M. (1998). DNA Double-stranded Breaks Induce Histone H2AX Phosphorylation on Serine 139. Journal of Biological Chemistry *273*, 5858–5868. 10.1074/jbc.273.10.5858.

49. Di Marco, S., Hasanova, Z., Kanagaraj, R., Chappidi, N., Altmannova, V., Menon, S., Sedlackova, H., Langhoff, J., Surendranath, K., Hühn, D., et al. (2017). RECQ5 Helicase Cooperates with MUS81 Endonuclease in Processing Stalled Replication Forks at Common Fragile Sites during Mitosis. Molecular Cell *66*, 658-671.e8. 10.1016/j.molcel.2017.05.006.

50. Chavdarova, M., Marini, V., Sisakova, A., Sedlackova, H., Vigasova, D., Brill, S.J., Lisby, M., and Krejci, L. (2015). Srs2 promotes Mus81–Mms4-mediated resolution of recombination intermediates. Nucleic Acids Research *43*, 3626–3642. 10.1093/nar/gkv198.

51. Cloud, V., Chan, Y.-L., Grubb, J., Budke, B., and Bishop, D.K. (2012). Rad51 Is an Accessory Factor for Dmc1-Mediated Joint Molecule Formation During Meiosis. Science *337*, 1222–1225. 10.1126/science.1219379.

52. Lv, W., Budke, B., Pawlowski, M., Connell, P.P., and Kozikowski, A.P. (2016). Development of Small Molecules that Specifically Inhibit the D-loop Activity of RAD51. J. Med. Chem. *59*, 4511–4525. 10.1021/acs.jmedchem.5b01762.

53. Branzei, D., and Szakal, B. (2016). DNA damage tolerance by recombination: Molecular pathways and DNA structures. DNA Repair *44*, 68–75. 10.1016/j.dnarep.2016.05.008.

54. Nayak, S., Calvo, J.A., Cong, K., Peng, M., Berthiaume, E., Jackson, J., Zaino, A.M., Vindigni, A., Hadden, M.K., and Cantor, S.B. (2020). Inhibition of the translesion synthesis polymerase REV1 exploits replication gaps as a cancer vulnerability. Sci. Adv. *6*, eaaz7808. 10.1126/sciadv.aaz7808.

55. Hodge, C.D., Spyracopoulos, L., and Glover, J.N.M. (2016). Ubc13: the Lys63 ubiquitin chain building machine. Oncotarget *7*, 64471–64504. 10.18632/oncotarget.10948.

56. Branzei, D. (2011). Ubiquitin family modifications and template switching. FEBS Letters *585*, 2810–2817. 10.1016/j.febslet.2011.04.053.

57. Fukushima, T., Matsuzawa, S., Kress, C.L., Bruey, J.M., Krajewska, M., Lefebvre, S., Zapata, J.M., Ronai, Z., and Reed, J.C. (2007). Ubiquitin-conjugating enzyme Ubc13 is a critical component of TNF receptor-associated factor (TRAF)-mediated inflammatory responses. Proc. Natl. Acad. Sci. U.S.A. *104*, 6371–6376. 10.1073/pnas.0700548104.

58. Ikura, T., Tashiro, S., Kakino, A., Shima, H., Jacob, N., Amunugama, R., Yoder, K., Izumi, S., Kuraoka, I., Tanaka, K., et al. (2007). DNA Damage-Dependent Acetylation and Ubiquitination of H2AX Enhances Chromatin Dynamics. Molecular and Cellular Biology *27*, 7028–7040. 10.1128/MCB.00579-07.

59. Vanoli, F., Fumasoni, M., Szakal, B., Maloisel, L., and Branzei, D. (2010). Replication and Recombination Factors Contributing to Recombination-Dependent Bypass of DNA Lesions by Template Switch. PLoS Genet *6*, e1001205. 10.1371/journal.pgen.1001205.

60. Osman, F., Dixon, J., Barr, A.R., and Whitby, M.C. (2005). The F-Box DNA Helicase Fbh1 Prevents Rhp51-Dependent Recombination without Mediator Proteins. Mol Cell Biol *25*, 8084–8096. 10.1128/MCB.25.18.8084-8096.2005.

61. Morishita, T., Furukawa, F., Sakaguchi, C., Toda, T., Carr, A.M., Iwasaki, H., and Shinagawa, H. (2005). Role of the *Schizosaccharomyces pombe* F-Box DNA Helicase in Processing Recombination Intermediates. Mol Cell Biol *25*, 8074–8083. 10.1128/MCB.25.18.8074-8083.2005.

62. Su, W.-P., Hsu, S.-H., Wu, C.-K., Chang, S.-B., Lin, Y.-J., Yang, W.-B., Hung, J.-J., Chiu, W.-T., Tzeng, S.-F., Tseng, Y.-L., et al. (2014). Chronic treatment with cisplatin induces replication-dependent sister chromatid recombination to confer cisplatin-resistant phenotype in nasopharyngeal carcinoma. Oncotarget *5*, 6323–6337. 10.18632/oncotarget.2210.

63. Hannay, J.A.F., Liu, J., Zhu, Q.-S., Bolshakov, S.V., Li, L., Pisters, P.W.T., Lazar, A.J.F., Yu, D., Pollock, R.E., and Lev, D. (2007). Rad51 overexpression contributes to chemoresistance in human soft tissue sarcoma cells: a role for p53/activator protein 2 transcriptional regulation. Molecular Cancer Therapeutics *6*, 1650–1660. 10.1158/1535-7163.MCT-06-0636.

64. Chen, G., Chen, J., Qiao, Y., Shi, Y., Liu, W., Zeng, Q., Xie, H., Shi, X., Sun, Y., Liu, X., et al. (2018). ZNF830 mediates cancer chemoresistance through promoting homologous-recombination repair. Nucleic Acids Research *46*, 1266–1279. 10.1093/nar/gkx1258.

65. Huang, W., Han, Z., Sun, Z., Feng, H., Zhao, L., Yuan, Q., Chen, C., Yu, S., Hu, Y., Yu, J., et al. (2022). PAK6 promotes homologous-recombination to enhance chemoresistance to oxaliplatin through ATR/CHK1 signaling in gastric cancer. Cell Death Dis *13*, 658. 10.1038/s41419-022-05118-8.

66. Mehta, K.P.M., Thada, V., Zhao, R., Krishnamoorthy, A., Leser, M., Lindsey Rose, K., and Cortez, D. (2022). CHK1 phosphorylates PRIMPOL to promote replication stress tolerance. Sci. Adv. *8*, eabm0314. 10.1126/sciadv.abm0314.

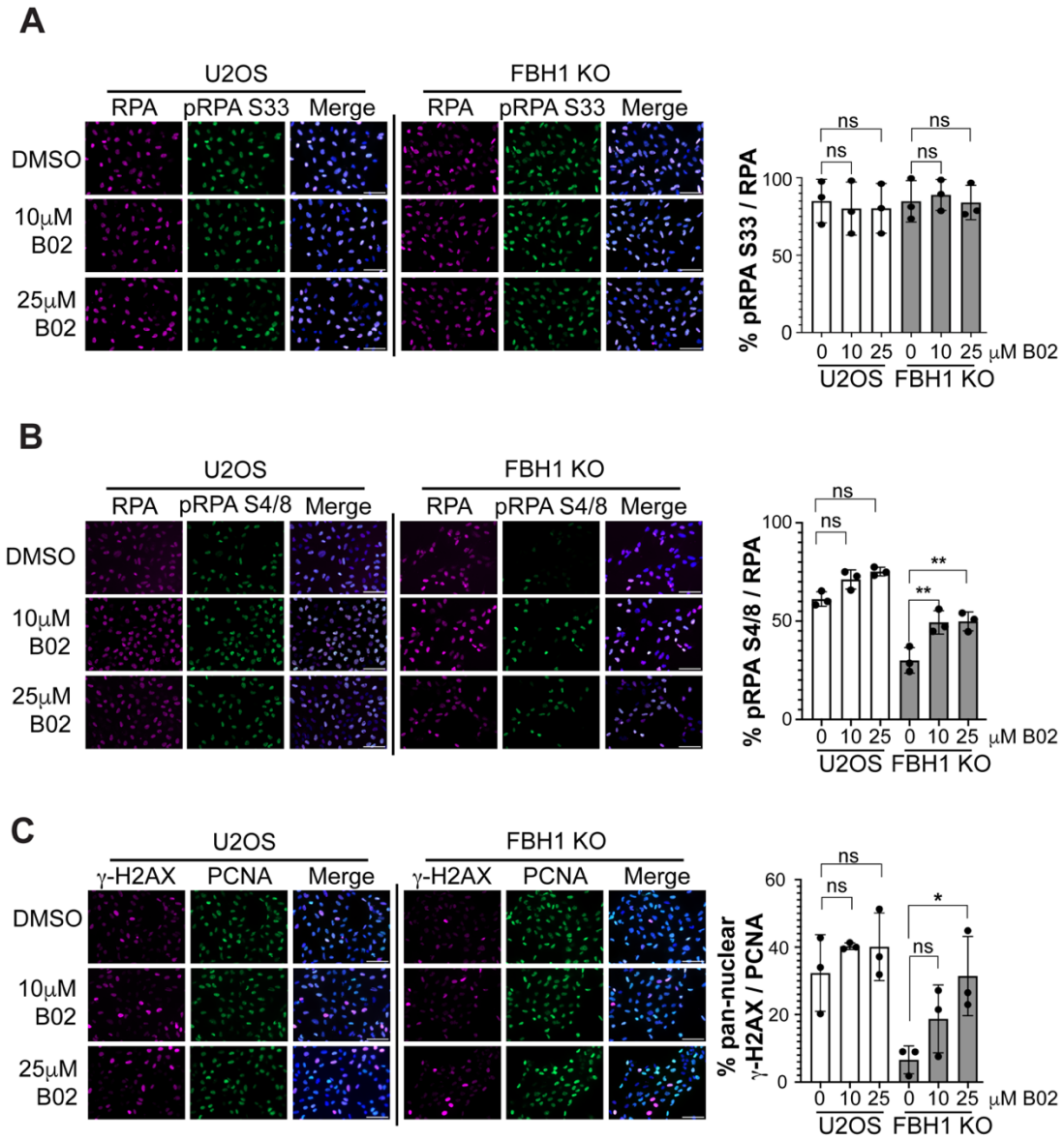

Figure 1. RAD51 DNA binding inhibition partially rescues DNA damage signaling in FBH1-KO cells. (A) Representative images of pRPA S33 (green) and RPA (magenta) in U2OS and FBH1 KO cells treated with 2mM HU +/- B02 for 24 hours. DNA is stained with DAPI (blue). Scale bar =100µm. Graph represents mean of three independent experiments. Error bars are standard deviation. Scale bar =100µm. **(B)** Representative images of pRPA S4/8 (green) and RPA (magenta) in U2OS and FBH1 KO cells treated with 2mM HU +/- B02 for 24 hours. DNA is stained with DAPI (blue). Scale bar =100µm. Graph represents mean of three independent experiments. Error bars are standard deviation. **(C)** Representative images of γ–H2AX (magenta) and PCNA (green) in U2OS and FBH1 KO cells treated with 2mM HU +/- B02 for 24 hours. DNA is stained with DAPI (blue) Scale bar =100µm. Graph represents mean of three independent experiments. Error bars are standard deviation. ns-not significant * $p<0.05$, ** $p<0.005$, Two-way ANOVA, Tukey.

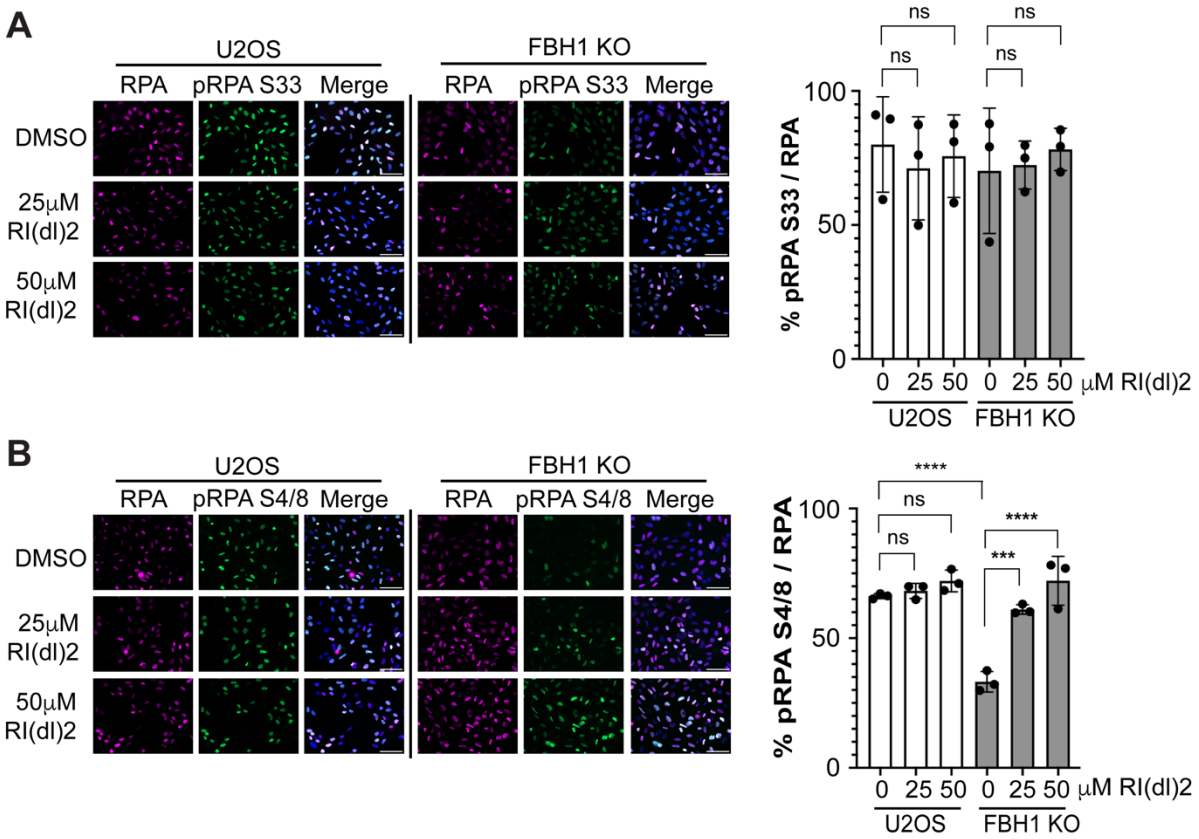

Figure 2. Inhibition of the strand exchange activity of RAD51 rescues DSB signaling in FBH1-KO cells. (A) Representative images of pRPA S33 (magenta) and RPA (green) in U2OS and FBH1 KO cells treated with 2mM HU +/- RI(dl)2 for 24 hours. DNA is stained with DAPI (blue). Scale bar =100µm. Graph represents mean of three independent experiments. Error bars are standard deviation. **(B)** Representative images of pRPA S4/8 (green) and RPA (magenta) in U2OS and FBH1 KO cells treated with 2mM HU +/- RI(dl)2 for 24 hours. DNA is stained with DAPI (blue). Scale bar =100µm. Graph represents mean of three independent experiments. Error bars are standard deviation. Error bars are standard deviation. ns – not significant. *** $p<0.0005$. **** $p<0.0001$. Two-way ANOVA, Tukey.

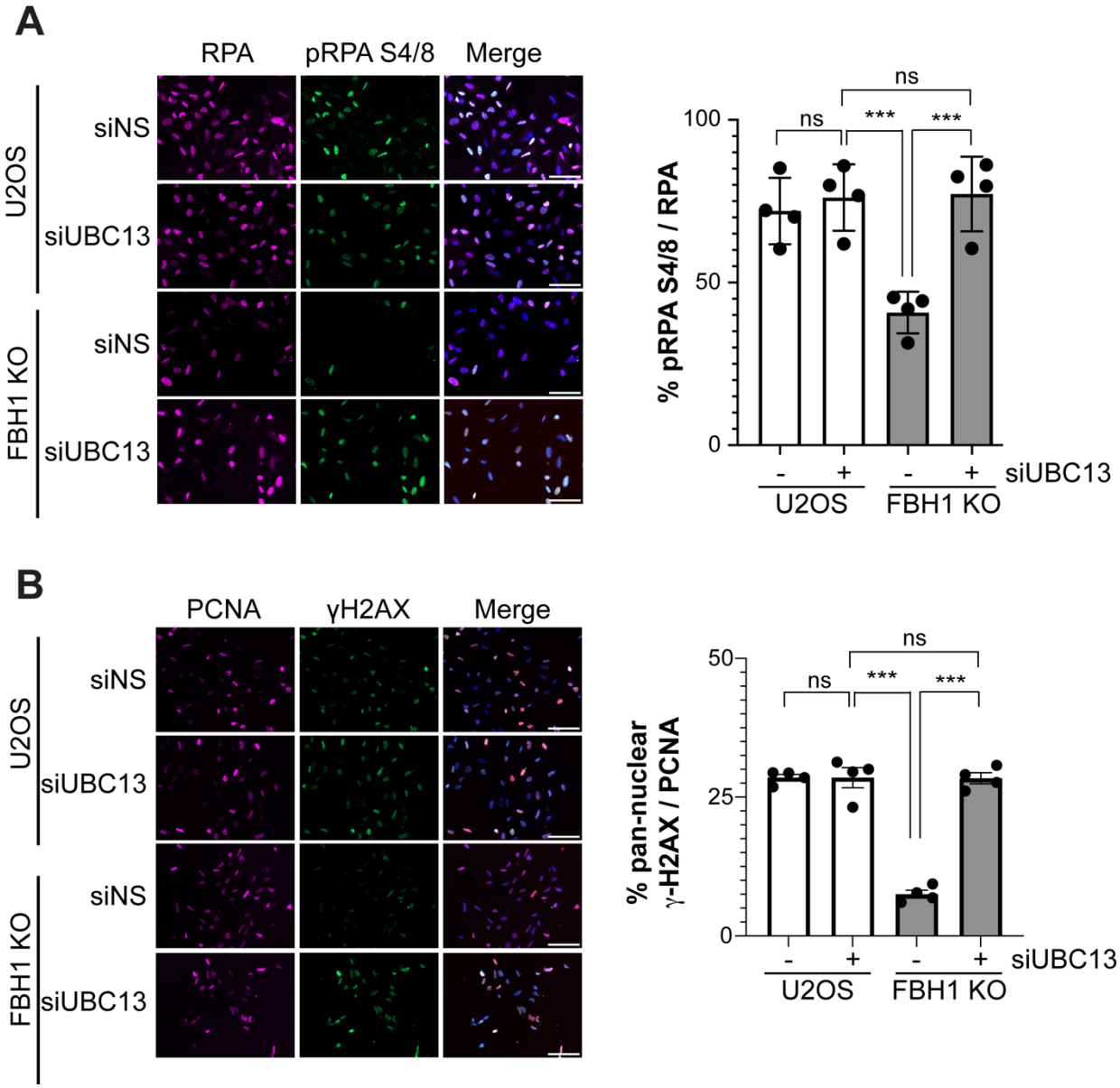

Figure 3. Depletion of UBC13 restores DSB signaling in FBH1-deficient cells. (A) Representative images of pRPA S4/8 (green) and RPA (magenta) in U2OS and FBH1 KO cells treated with 2mM HU for 24 hours. DNA is stained with DAPI (blue). Scale bar = 100µm. Graph represents mean of four independent experiments. Error bars are standard deviation. **(B)** Representative images of γ-H2AX (green) and PCNA (magenta) in U2OS and FBH1 KO cells treated with 2mM HU for 24 hours. DNA is stained with DAPI (blue). Scale bar =100µm. Graph represents mean of four independent experiments. Error bars are standard deviation. ns – not significant. ***p<0.0005, **** p<0.0001, Two-way ANOVA, Tukey.

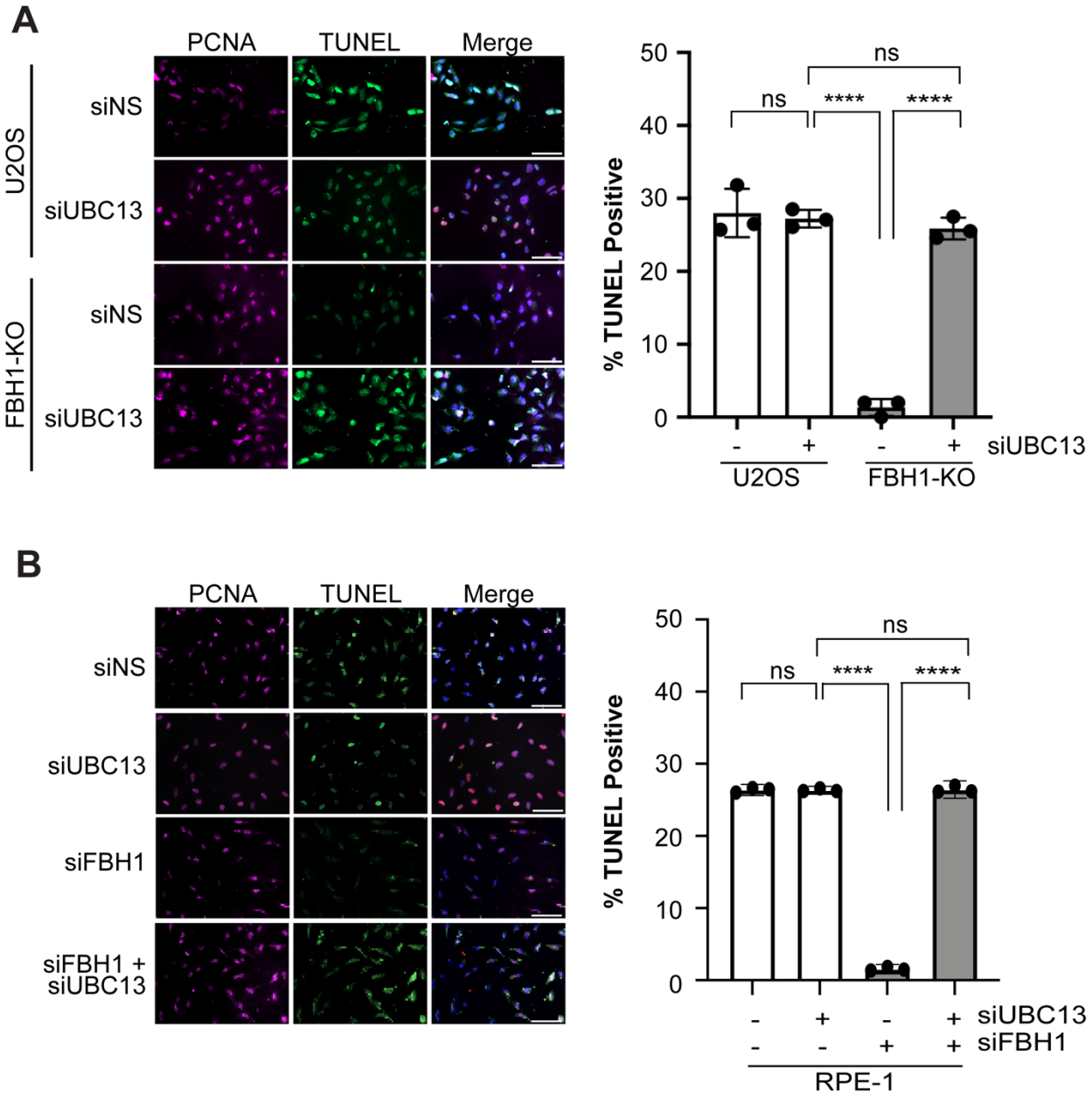

Figure 4: UBC13 depletion increases DSB formation in FBH1-deficient cells. (A) Representative images of TUNEL (green) and PCNA (magenta) in U2OS and FBH1 KO cells after treatment with 2 mM HU. DNA is stained with DAPI (blue). Graph represents mean of three independent experiments. Error bars are standard deviation. Scale bar =100 µm. **(B)** Representative images of TUNEL (Green) and PCNA (magenta) in RPE-1 cells transfected with the indicated siRNAs. DNA is stained with DAPI (blue). Scale bar =100 µm. Graph represents mean of three independent experiments. Error bars are standard deviation. Scale bar =100 µm. ns – not significant, **** - $p<0.0001$, Two-way ANOVA, Tukey.

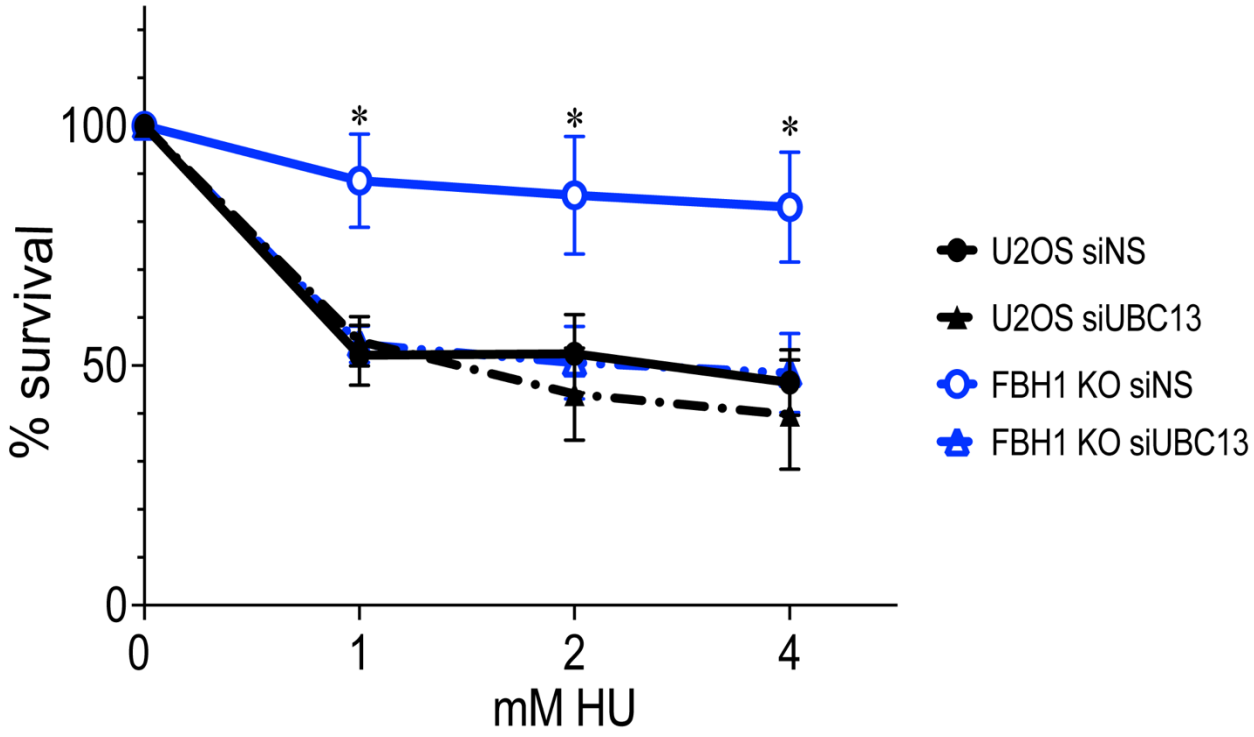

Figure 5. Depletion of UBC13 sensitizes FBH1-deficient cells to HU. Quantification of cellular survival in U2OS and FBH1 KO cells after treatment with indicated HU concentrations. Line represents average of three independent experiments. Error bars are standard error. *$p<0.05$, ANOVA, t-test.

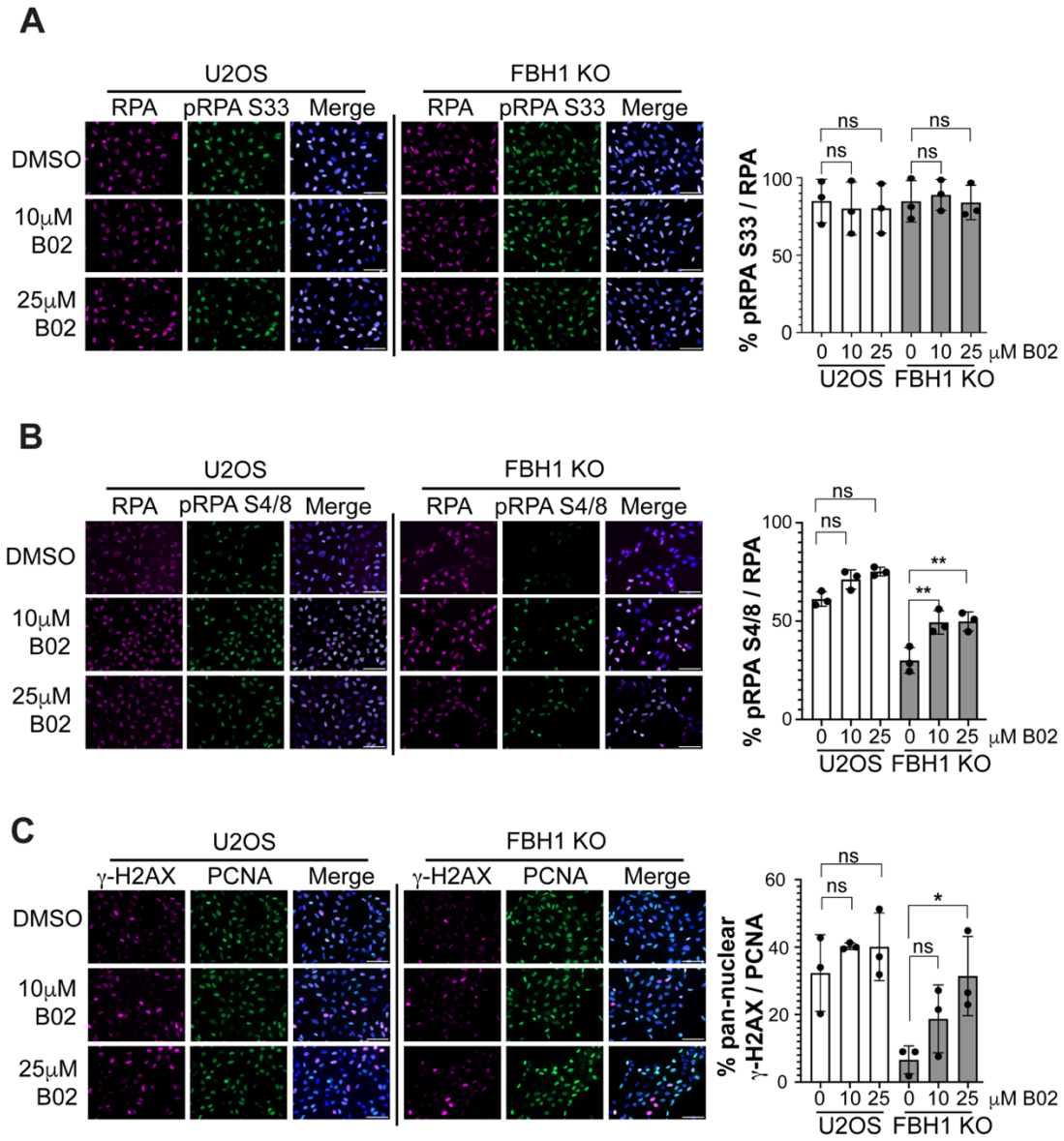

Figure 1. RAD51 DNA binding inhibition partially rescues DNA damage signaling in FBH1-KO cells. (A) Representative images of pRPA S33 (green) and RPA (magenta) in U2OS and FBH1 KO cells treated with 2mM HU +/- B02 for 24 hours. DNA is stained with DAPI (blue). Scale bar =100µm. Graph represents mean of three independent experiments. Error bars are standard deviation. Scale bar =100µm. **(B)** Representative images of pRPA S4/8 (green) and RPA (magenta) in U2OS and FBH1 KO cells treated with 2mM HU +/- B02 for 24 hours. DNA is stained with DAPI (blue). Scale bar =100µm. Graph represents mean of three independent experiments. Error bars are standard deviation. **(C)** Representative images of γ–H2AX (magenta) and PCNA (green) in U2OS and FBH1 KO cells treated with 2mM HU +/- B02 for 24 hours. DNA is stained with DAPI (blue) Scale bar =100µm. Graph represents mean of three independent experiments. Error bars are standard deviation. ns-not significant * $p<0.05$, ** $p<0.005$, Two-way ANOVA, Tukey.

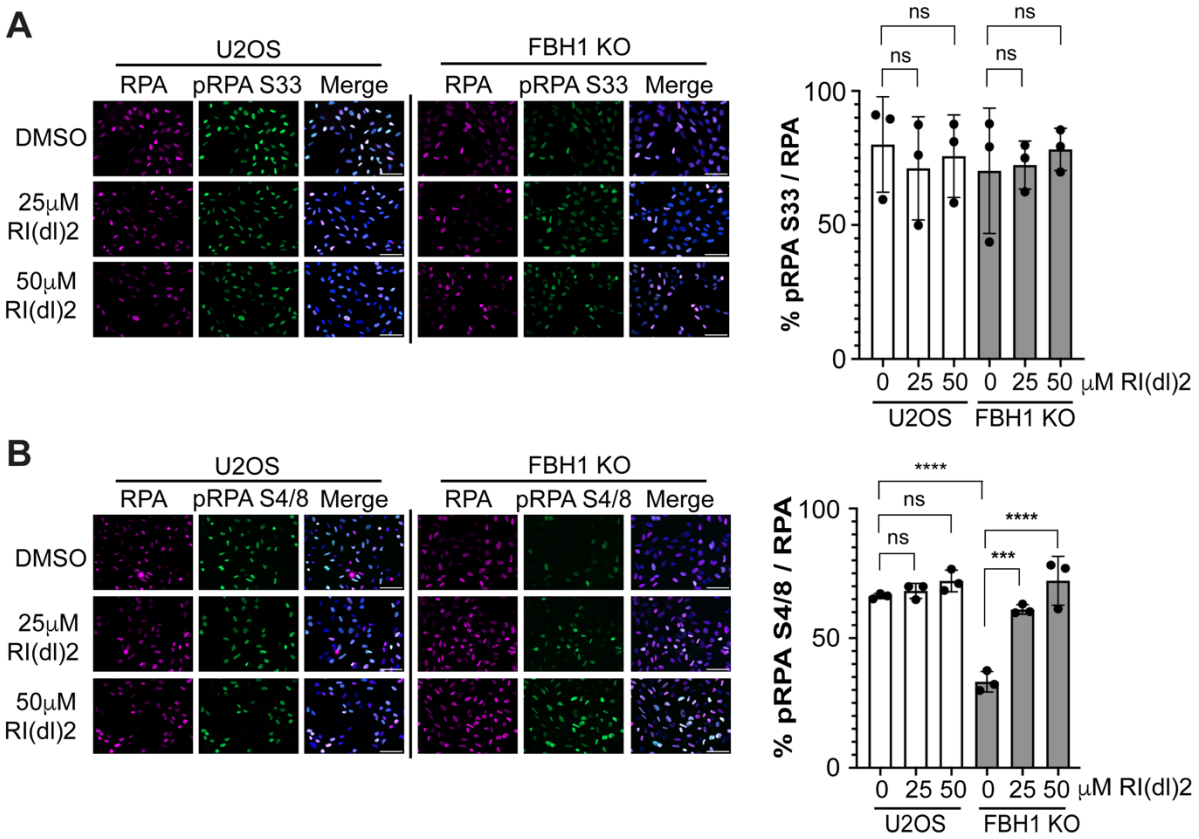

Figure 2. Inhibition of the strand exchange activity of RAD51 rescues DSB signaling in FBH1-KO cells. (A) Representative images of pRPA S33 (magenta) and RPA (green) in U2OS and FBH1 KO cells treated with 2mM HU +/- RI(dl)2 for 24 hours. DNA is stained with DAPI (blue). Scale bar =100µm. Graph represents mean of three independent experiments. Error bars are standard deviation. **(B)** Representative images of pRPA S4/8 (green) and RPA (magenta) in U2OS and FBH1 KO cells treated with 2mM HU +/- RI(dl)2 for 24 hours. DNA is stained with DAPI (blue). Scale bar =100µm. Graph represents mean of three independent experiments. Error bars are standard deviation. Error bars are standard deviation. ns – not significant. *** $p<0.0005$. **** $p<0.0001$. Two-way ANOVA, Tukey.

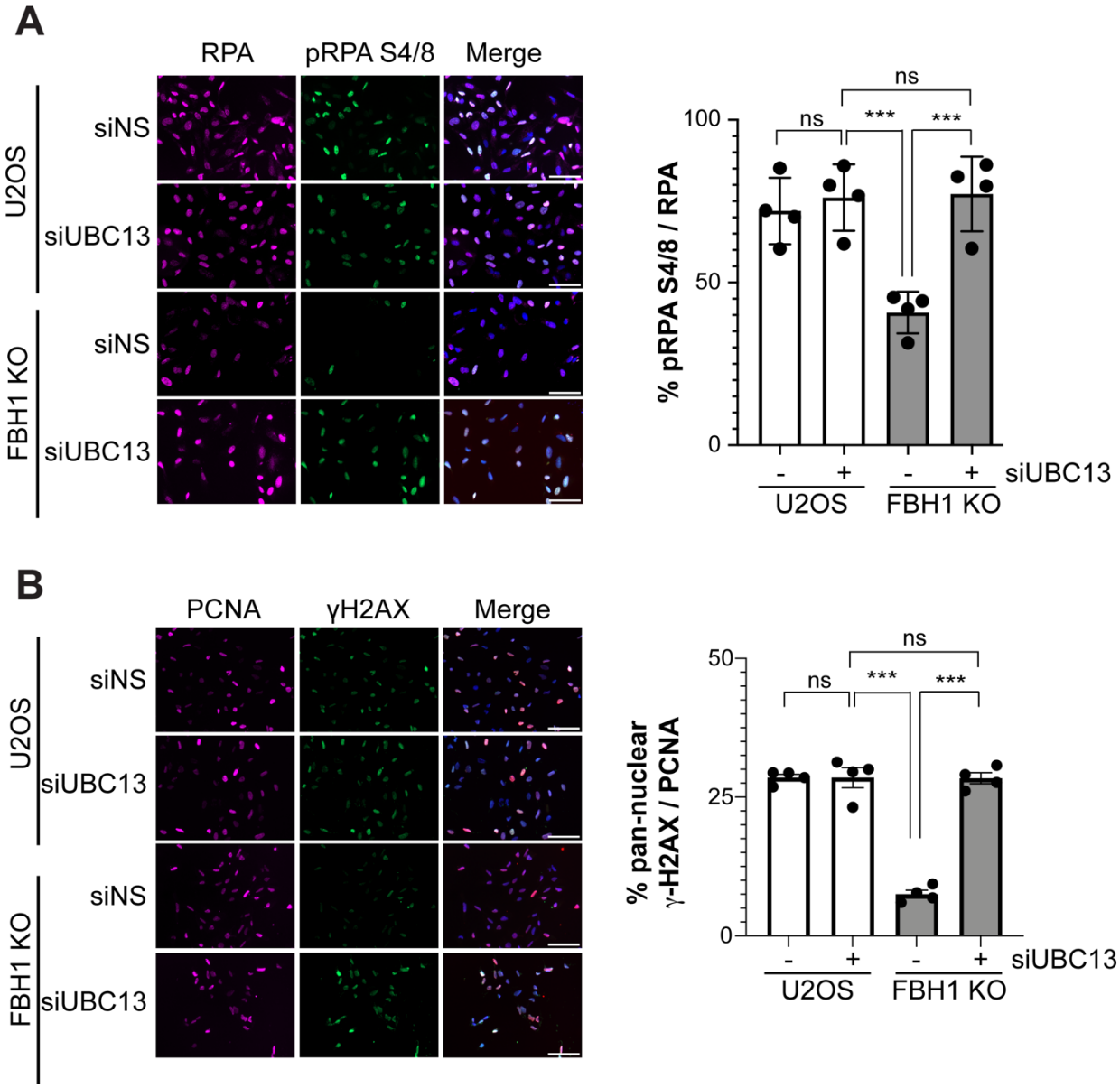

Figure 3. Depletion of UBC13 restores DSB signaling in FBH1-deficient cells. (A) Representative images of pRPA S4/8 (green) and RPA (magenta) in U2OS and FBH1 KO cells treated with 2mM HU for 24 hours. DNA is stained with DAPI (blue). Scale bar = 100µm. Graph represents mean of four independent experiments. Error bars are standard deviation. **(B)** Representative images of γ-H2AX (green) and PCNA (magenta) in U2OS and FBH1 KO cells treated with 2mM HU for 24 hours. DNA is stained with DAPI (blue). Scale bar =100µm. Graph represents mean of four independent experiments. Error bars are standard deviation. ns – not significant. ***p<0.0005, **** p<0.0001, Two-way ANOVA, Tukey.

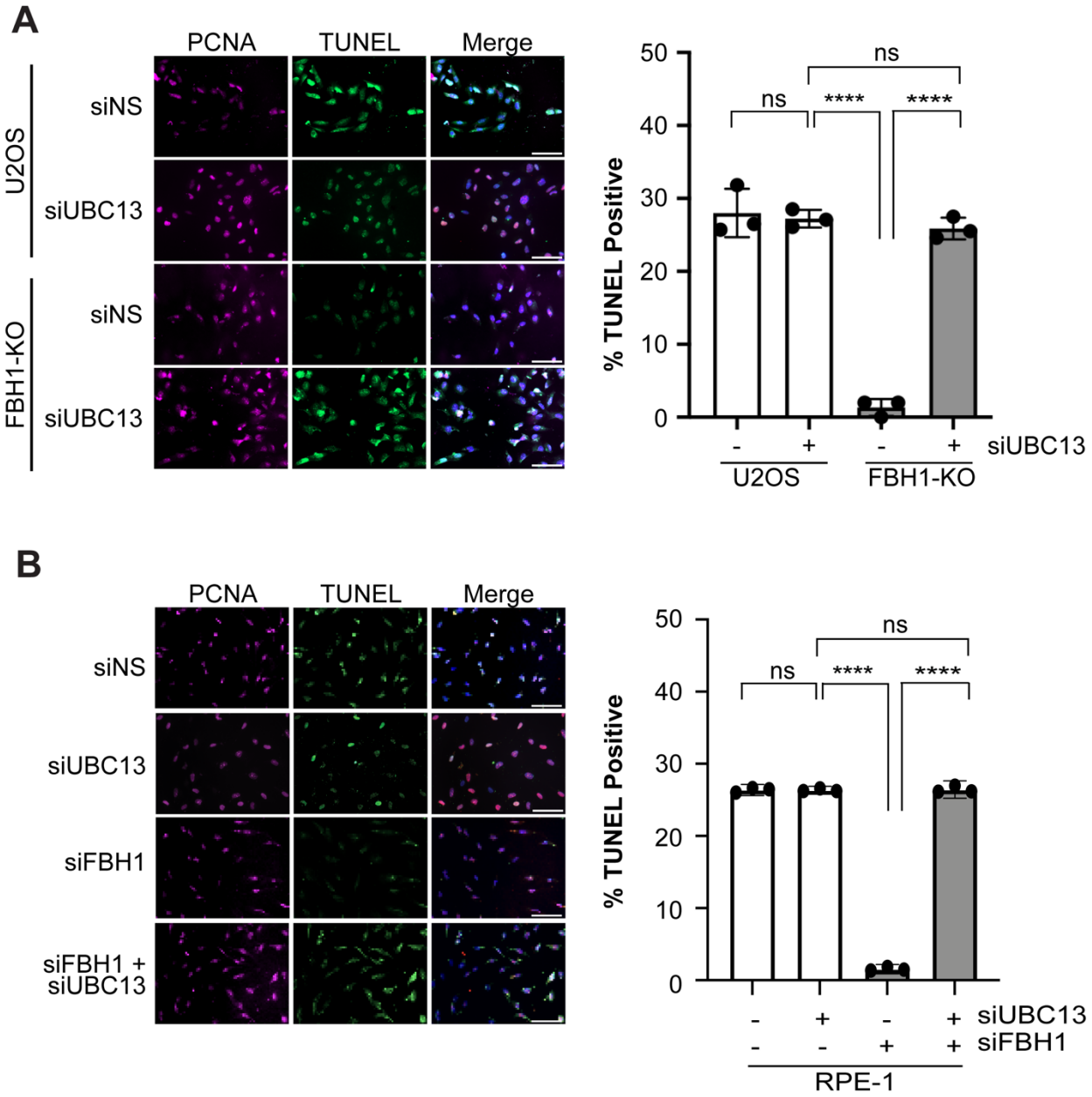

Figure 4: UBC13 depletion increases DSB formation in FBH1-deficient cells. (A) Representative images of TUNEL (green) and PCNA (magenta) in U2OS and FBH1 KO cells after treatment with 2 mM HU. DNA is stained with DAPI (blue). Graph represents mean of three independent experiments. Error bars are standard deviation. Scale bar =100 µm. **(B)** Representative images of TUNEL (Green) and PCNA (magenta) in RPE-1 cells transfected with the indicated siRNAs. DNA is stained with DAPI (blue). Scale bar =100 µm. Graph represents mean of three independent experiments. Error bars are standard deviation. Scale bar =100 µm. ns – not significant, **** - $p<0.0001$, Two-way ANOVA, Tukey.

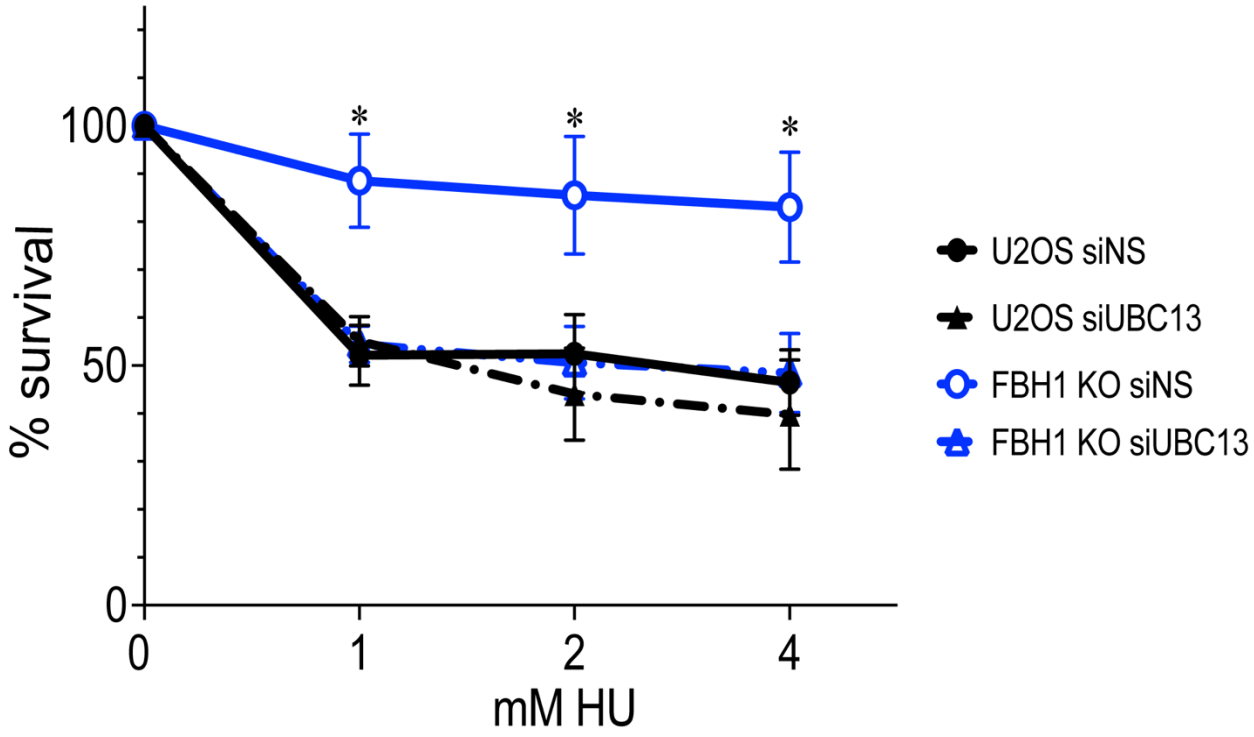

Figure 5. Depletion of UBC13 sensitizes FBH1-deficient cells to HU. Quantification of cellular survival in U2OS and FBH1 KO cells after treatment with indicated HU concentrations. Line represents average of three independent experiments. Error bars are standard error. *$p<0.05$, ANOVA, t-test.

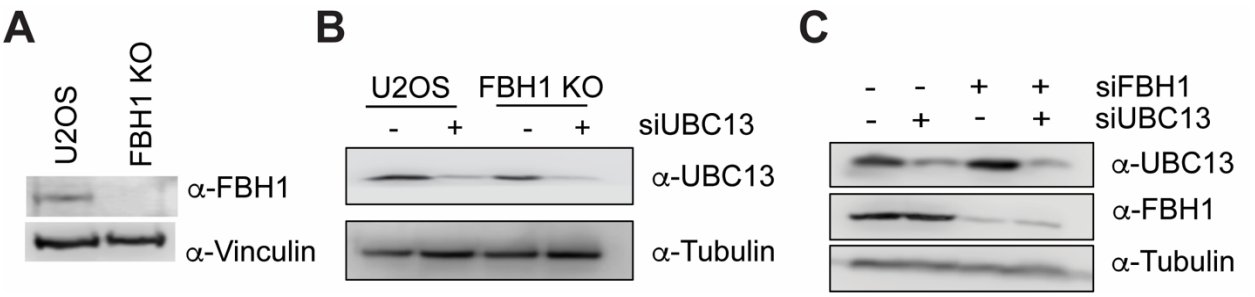

Supplemental Figure 1. FBH1 protein levels in indicated cell lines (A) Western blot showing FBH1 levels in U2OS and FBH1 KO cells. (B) Western blot showing UBC13 knockdown in U2OS and FBH1 KO cells. (C) Western blot showing UBC13 and FBH1 knockdown in RPE-1 cells.

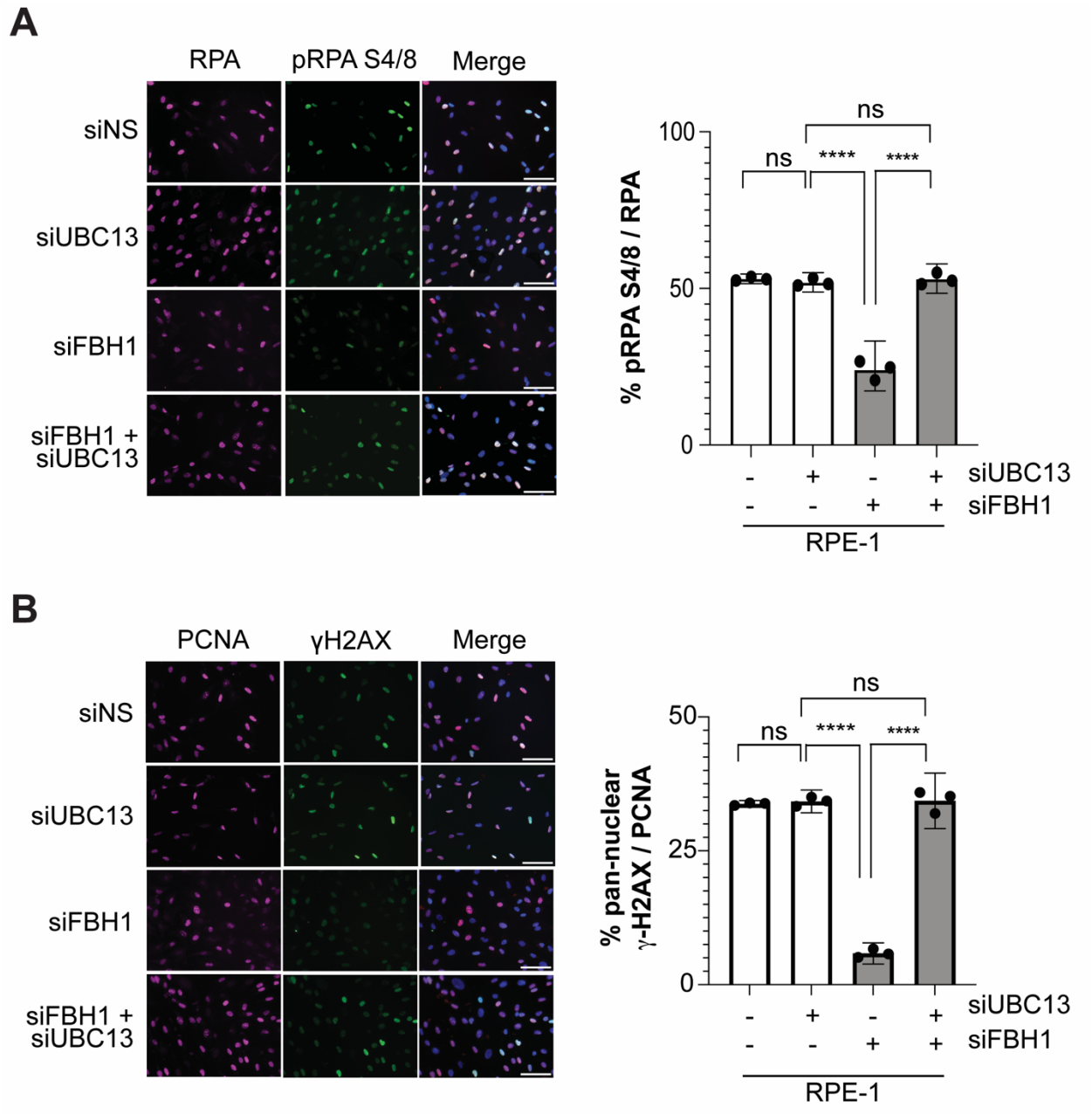

Supplemental Figure 2. Depletion of UBC13 restores DSB signaling in RPE-1 cells. (A) Representative images of pRPA S4/8 (green) and RPA (magenta) in RPE-1 cells treated with 2mM HU after transfection with the indicated siRNAs. DNA is stained with DAPI (blue). Scale bar =100µm. Graph represents mean of three independent experiments. Error bars are standard deviation. **(B)** Representative images of γ-H2AX (green) and PCNA (magenta) in RPE-1 cells treated with 2mM HU after transfection with the indicated siRNAs. DNA is stained with DAPI (blue) Scale bar =100µm. Graph represents mean of three independent experiments. Error bars are standard deviation. ns – not significant. **** - $p<0.0001$. Two-way ANOVA, Tukey.